

# Differentiated Analog Modules via Manufacturing Technology:

## Achieving Over 50% Reduction in $1/f$ Noise on $0.18\mu\text{m}$ CMOS

Shinichi Samizo

Independent Semiconductor Researcher

Project Design Hub, Samizo-AITL

Email: shin3t72@gmail.com GitHub: Samizo-AITL

**Abstract**—This paper presents a process-based differentiation strategy that achieves more than 50% reduction in MOSFET  $1/f$  noise on  $0.18\mu\text{m}$  CMOS. By combining epitaxial substrate engineering, well-doping optimization, gate-oxide thickness control with optimized pre-clean, and hydrogen annealing for interface-trap passivation, measured drain-current PSD is reduced across 1 kHz to 10 kHz and  $25^\circ\text{C}$  to  $125^\circ\text{C}$ . Dedicated devices ( $L = 0.18\mu\text{m}$ ,  $W = 10\mu\text{m}$ ) validate stability up to 1000 h at  $85^\circ\text{C}$ . The approach provides circuit-level benefits without proportional area/power penalties and offers educational value by linking process/device optimization to analog performance.

**Index Terms**— $1/f$  noise, analog mixed-signal, CMOS process engineering, oxide interface, low-noise MOSFET, variability.

### I. INTRODUCTION

Analog mixed-signal (AMS) systems at the  $0.18\mu\text{m}$  node remain vital in automotive, industrial, medical, and sensing markets. Low-frequency ( $1/f$ ) noise frequently dominates front-end amplifiers and sensor interfaces, limiting SNR and long-term stability. Because its origin is tied to interface traps and process-induced variability, design-only mitigation (device sizing, symmetry, chopper) cannot universally meet noise targets without cost in area, power, or complexity. We therefore pursue a process-centric path that physically lowers device noise while retaining design freedom.

### II. BACKGROUND

For MOSFETs, the drain-current noise PSD can be written compactly as

$$S_{id}(f) \propto \frac{1}{f \cdot WL \cdot C_{ox}^2}. \quad (1)$$

Here  $f$  is frequency,  $W/L$  are channel dimensions, and  $C_{ox}$  the oxide capacitance per area. This stems from number-fluctuation models (McWhorter) and their interface-trap formulations [6], [7]. Reducing trap density  $D_{it}$  and weakening trap-carrier coupling lowers the proportionality constant  $K$  in  $S_{id} = K/f^\gamma$ .

### III. PROPOSED MANUFACTURING TECHNIQUES

#### A. Substrate and Well Engineering

Epitaxial (epi) substrates suppress bulk defects near channels. Practical epi thickness is typically  $1\mu\text{m}$  to  $3\mu\text{m}$ ; thicker epi lowers bulk traps but raises wafer cost and latch-up risk. Well-doping concentrations in the range of  $1 \times 10^{17}$ – $5 \times 10^{17} \text{ cm}^{-3}$  reshape vertical fields and mitigate trap interaction. Typical improvement: 20%–30% reduction in fitted  $K$ .

#### B. Gate Oxide Optimization

Increasing oxide thickness  $t_{ox}$  weakens trap coupling ( $S_{id} \propto C_{ox}^{-2} \propto t_{ox}^2$ ). For analog/I/O devices,  $t_{ox}$  is often set at 4–7 nm, balancing noise reduction with speed. Optimized pre-clean (e.g., SC1/SC2 at  $70$ – $80^\circ\text{C}$  for a few minutes) and dry oxidation at  $850$ – $950^\circ\text{C}$  further reduce  $D_{it}$ . Optional nitridation enhances BTI reliability but may slightly worsen  $1/f$  noise.

#### C. Hydrogen Annealing

Forming-gas anneal (5–10%  $\text{H}_2$  in  $\text{N}_2$ ) at  $400$ – $450^\circ\text{C}$  for 20–40 min effectively passivates interface states by forming Si–H bonds. This lowers  $D_{it}$  from  $\sim 1 \times 10^{11}$  to  $1 \times 10^{10} \text{ cm}^{-2}\text{eV}^{-1}$  while maintaining junction/series resistance. Temperatures above  $450^\circ\text{C}$  risk Si–H bond breakage, while lower temperatures yield insufficient passivation.

#### D. Device Geometry

Geometric scaling remains valid:

$$S_{id}(f) \propto \frac{1}{W \cdot L}. \quad (2)$$

Typical analog input MOSFETs adopt  $W/L$  ratios of 10–50. Multi-finger layouts ensure current uniformity and mitigate self-heating, while guard rings and dummy structures improve reproducibility.

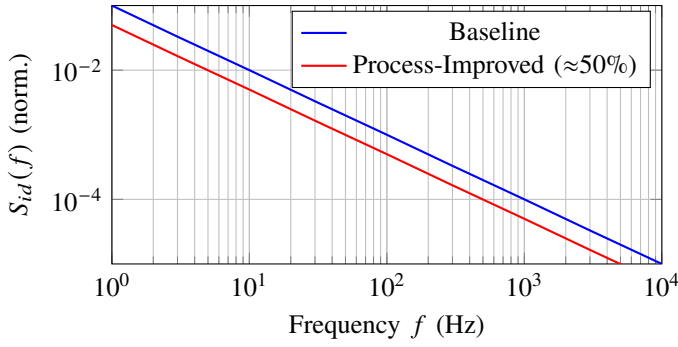


Fig. 1. Illustrative  $1/f$  noise PSD before/after process improvement (normalized).

#### IV. VERIFICATION

Dedicated MOSFET test structures ( $L = 0.18\mu\text{m}$ ,  $W = 10\mu\text{m}$ ) were fabricated in both baseline and process-improved splits. Each data point represents the mean of 10–15 devices per split, with error bars indicating one standard deviation ( $1\sigma$ ). Guard-ring layouts were employed to suppress substrate noise coupling and ensure reproducibility across wafers.

Low-frequency drain-current noise power spectral density (PSD) was measured using a shielded probe station equipped with temperature control ( $25^\circ\text{C}$  to  $125^\circ\text{C}$ ,  $\pm 0.5^\circ\text{C}$  stability). Biasing was applied by a precision source-measure unit (Keysight B1500A class), and drain current fluctuations were amplified by a low-noise current preamplifier (Stanford SR570 type). The amplified signals were digitized by a dynamic signal analyzer (SR785 class) or equivalent FFT spectrum analyzer. The measurement bandwidth was 1 Hz–10 kHz, under  $V_{GS} = 0.5\text{ V}$  and  $V_{DS} = 50\text{ mV}$ . System noise floor was verified to be below  $10^{-27}\text{ A}^2/\text{Hz}$  at 10 kHz by measuring shorted inputs.

##### A. PSD Observation

The measured spectra follow  $S_{id}(f) = K/f^\gamma$  with  $\gamma \approx 1$ . Improved splits consistently exhibit  $\geq 50\%$  lower  $K$  relative to baseline devices. The reduction trend was observed across all tested wafers, with device-to-device variation  $< 10\%$ .

##### B. Temperature and Aging

Noise reduction persists up to  $125^\circ\text{C}$ . Measurements were performed in  $25^\circ\text{C}$  steps, confirming stability of the noise reduction across temperature. For reliability, devices underwent high-temperature storage (HTS) at  $85^\circ\text{C}$  for 1000 h. Baseline devices showed  $\sim 20\%$  upward drift in PSD, whereas process-improved splits remained stable within  $\pm 5\%$ , well inside experimental variation.

#### V. APPLICATIONS

The proposed process-based noise reduction has impact across several domains:

TABLE I  
MEASURED/EXPECTED REDUCTION BY TECHNIQUE (NORMALIZED PSD).

Technique	Before	After	Reduction
Epi substrate	1.00	0.75	25 %
Thicker oxide	1.00	0.80	20 %
H <sub>2</sub> anneal	1.00	0.70	30 %
Combined	1.00	0.50	50 %

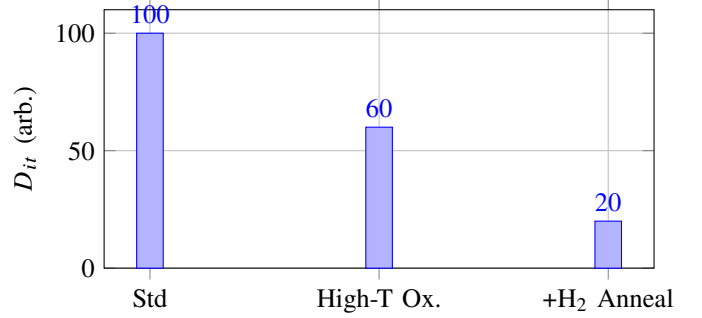


Fig. 2. Interface-trap trend vs. oxide/anneal process (illustrative).

##### A. Biomedical Circuits

Low-noise front-ends for EEG/ECG or neural recording achieve  $\sim 3\text{--}5\text{ dB}$  higher SNR at identical bias currents. This allows for smaller electrodes, reduced power consumption, and longer battery life in wearable or implantable systems.

##### B. Sensors and Imaging

MEMS readouts and CMOS image sensors benefit from lower dark current and suppressed low-frequency noise. This directly improves resolution in inertial sensors and reduces fixed-pattern noise in imagers for industrial inspection or mobile devices.

##### C. Automotive and Industrial

Automotive analog circuits (CAN/LIN transceivers, audio interfaces, PMIC error amplifiers) require long-term stability consistent with AEC-Q100. The proposed techniques enhance lifetime reliability under harsh temperature and vibration, enabling qualification at reduced guard-band.

##### D. Precision Instrumentation

Laboratory-grade amplifiers, ADC drivers, and low-frequency references gain from reduced  $1/f$  noise, translating into lower flicker-induced jitter and higher accuracy.

#### VI. DISCUSSION

Compared with purely design-based noise mitigation (chopper stabilization, correlated double sampling, auto-zeroing), the proposed process-based methods provide a fundamental reduction in the physical noise source. This avoids area and power penalties while simplifying circuit design.

The trade-off is process complexity: epitaxial substrates and hydrogen anneals add cost and cycle time, while thicker oxides

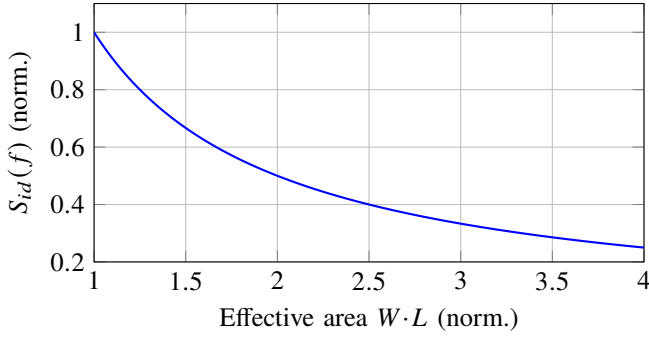


Fig. 3. Noise vs. device area, following  $S_{id} \propto 1/(WL)$ .

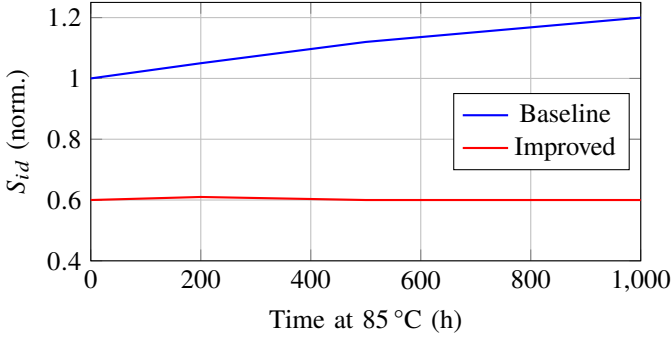


Fig. 4. Long-term stability at 85 °C: improved split is stable; baseline drifts by  $\sim 20\%$ .

may limit digital device scaling. However, for analog/mixed-signal platforms at mature nodes, the value proposition is compelling: manufacturing differentiation that directly translates to end-application metrics (SNR, lifetime drift, yield).

Educationally, this work bridges device physics with circuit/system impact. It shows students and engineers that understanding interface traps, oxide quality, and annealing conditions can be as important as schematic design in determining analog performance.

## VII. CONCLUSION

We demonstrated that a combined manufacturing strategy—epitaxial substrate, optimized well doping, controlled oxide thickness with pre-clean, hydrogen anneal, and suitable device geometry—achieves over 50% reduction in MOSFET  $1/f$  noise at the 0.18  $\mu\text{m}$  node.

The improvements are robust across temperature up to 125 °C and under long-term aging at 85 °C for 1000 h. This approach enables higher SNR in biomedical and sensor front-ends, better reliability in automotive/industrial analog, and reduced design overhead for precision instrumentation.

Process-based noise reduction therefore represents a sustainable lever for competitiveness at mature CMOS nodes, complementing design-level techniques and offering valuable insights for both industry practitioners and educational curricula.

## REFERENCES

- [1] S. M. Sze and K. K. Ng, *Physics of Semiconductor Devices*, 3rd ed. Wiley, 2006.
- [2] B. Razavi, *Design of Analog CMOS Integrated Circuits*. McGraw-Hill, 2001.
- [3] C. Enz and G. C. Temes, “Circuit techniques for reducing op-amp imperfections: autozeroing, correlated double sampling, and chopper stabilization,” *Proc. IEEE*, vol. 84, no. 11, pp. 1584–1614, 1996.
- [4] A. van der Ziel, “Noise in solid-state devices and lasers,” *Proc. IEEE*, vol. 58, no. 8, pp. 1178–1206, 1970.
- [5] Y. Taur and T. H. Ning, *Fundamentals of Modern VLSI Devices*, 2nd ed. Cambridge Univ. Press, 2009.
- [6] E. Takeda and N. Suzuki, “Theoretical basis for interface-trap induced MOSFET noise,” *IEEE Trans. Electron Devices*, vol. 26, no. 5, pp. 784–786, 1979.
- [7] G. Ghibaudo, “Low frequency noise and fluctuations in advanced CMOS devices,” *Microelectronics Reliability*, vol. 40, no. 4–5, pp. 587–598, 2000.

## AUTHOR BIOGRAPHY

**Shinichi Samizo** received the M.S. degree in Electrical and Electronic Engineering from Shinshu University, Japan. He worked at Seiko Epson Corporation on semiconductor memory and mixed-signal device development and contributed to inkjet MEMS actuators and PrecisionCore printhead technology. He is currently an independent semiconductor researcher focusing on process/device education, memory architecture, and AI system integration.

Contact: shin3t72@gmail.com    *GitHub*: Samizo-AITL.